

Spectral diffusion of phosphorus donors in silicon at high magnetic field

Lihuang Zhu,¹ Johan van Tol,² and Chandrasekhar Ramanathan^{3,*}

¹Lam Research Corporation, Fremont, California 94538, USA

²National High Magnetic Field Laboratory, Tallahassee, Florida 32310, USA

³Dartmouth College, Hanover, New Hampshire 03755, USA

(Dated: July 15, 2021)

We characterize the phase memory time of phosphorus donor electron spins in lightly-doped natural silicon at high magnetic field (8.58 T) in the dark and under low-power optical excitation. The spin echo decays are dominated by spectral diffusion due to the presence of the 4.7 % abundant spin-1/2 silicon-29 nuclei. At 4.2 K, the spectral diffusion time (T_{SD}) measured in the dark is $124 \pm 7 \mu\text{s}$, a factor of 2 smaller than that measured at low magnetic fields (0.35 T). Using a tunable laser we also measured the echo decay as the wavelength of the optical excitation is swept across the band edge from 1050 nm to 1090 nm. Above-bandgap optical excitation is seen to *increase* the spectral diffusion time of the donor electron spin to $201 \pm 11 \mu\text{s}$. The physical mechanism underlying both the decrease of T_{SD} at high field and the subsequent increase under optical excitation remains unclear.

Donor and defect electronic spins in solids are promising platforms for quantum technologies [1, 2]. Understanding how systems such as donors in silicon or defects in diamond and silicon carbide decohere under different experimental conditions is key to enabling improved materials design and to identifying optimal operating conditions.

The donor electrons in phosphorus-doped silicon (Si:P) have some of the longest coherence times observed in solid-state spin systems [3, 4]. Natural silicon consists of 3 isotopes: ^{28}Si , ^{29}Si and ^{30}Si , whose relative abundances are 92.23%, 4.67% and 3.1% respectively. While ^{29}Si is a spin-1/2 nucleus, ^{28}Si and ^{30}Si are spin-0 nuclei. Spectral diffusion due to the ^{29}Si spins is the dominant source of spin echo decay in lightly-doped natural Si:P samples at and below 4 K in low magnetic fields [4–9]. The spin dynamics of the isolated donor spin are determined by its hyperfine interactions with surrounding nuclear spins – an instance of the classic central spin problem [10]. Many-body magnetic dipolar interactions between the nuclear spins induce a fluctuating nuclear magnetic field at the site of the donor electron spin causing the echo decay [11]. The elimination of the spin-1/2 ^{29}Si nuclei was seen to dramatically suppress spectral diffusion of the phosphorus donor electron resonance in low-field experiments [4], enabling the development of coherent single and two-qubit devices [12–16].

Here we measure the phase memory time of the donor electron in a lightly-doped ($N_D = 3.3 - 3.5 \times 10^{15} \text{ cm}^{-3}$) natural abundance Si:P sample at liquid helium temperatures at 8.58 T, both in the dark and with low power optical excitation. The experiments were performed on the 240 GHz electron magnetic resonance setup at the National High Field Magnet Laboratory (NHFML) [17].

At low donor concentrations, the Hamiltonian of the isolated phosphorus donor at high magnetic field is

$$H = \omega_e S_z + \omega_P I_z^P + \frac{2\pi}{\hbar} A S_z I_z^P \quad (1)$$

which results in two electron spin resonance (ESR) tran-

sitions at frequencies $\nu_e \pm A/2$. Figure 1(a) shows the continuous wave ESR spectrum of the sample with the two hyperfine-split transitions separated by 4.2 mT (117.5 MHz). The small central peak is due to contributions from coupled donor pairs [18, 19]. The intensity of the two ESR transitions are nearly equal, indicating a low polarization of the ^{31}P nuclear spins. As these two transitions are well separated in energy, it is possible to address and measure their coherence times individually.

Figure 1(b) shows the measured echo decay in the dark (red) and with 1051 nm ($E = 1.18 \text{ eV}$) optical excitation (blue). The optical excitation is clearly seen to extend the timescale of the signal decays. This is a surprising effect as optical excitation – though typically at higher intensities – has been shown to dramatically reduce both T_1 and T_2 relaxation times for donors in silicon [20–22]. Each data point is an average over 16 scans. The signal intensity is calculated from the total area of the echo using both in-phase and quadrature channels.

The inset to the figure shows a schematic of the two-pulse spin echo experiment. The durations of the $\pi/2$ and π pulses were 500 ns and 980 ns respectively. The echo delay τ was incremented from 2 μs to 100 μs in 2 μs steps. The repetition time of the experiment was set to 1 s, which is much longer than the electron spin T_1 ($\sim 20 \text{ ms}$ [23]), but still short compared to any nuclear spin T_1 time (typically several hours [24]). Laser excitation (when used) was applied continuously to the sample throughout the experiment. The echo decay measured in the dark was acquired immediately after the conclusion of the experiment with optical illumination. The size of the Si:P sample was about $5 \times 5 \times 3 \text{ mm}$. The orientation of the crystal in the magnetic field is unknown in our experiments.

In general, there are different phenomena that contribute to the decay of a spin echo signal in systems such as Si:P. The echo intensity at time 2τ

$$S(2\tau) = S_0 e^{-2\tau/T_{1D}} e^{-2\tau/T_2} e^{-(2\tau/T_{SD})^n} \quad (2)$$

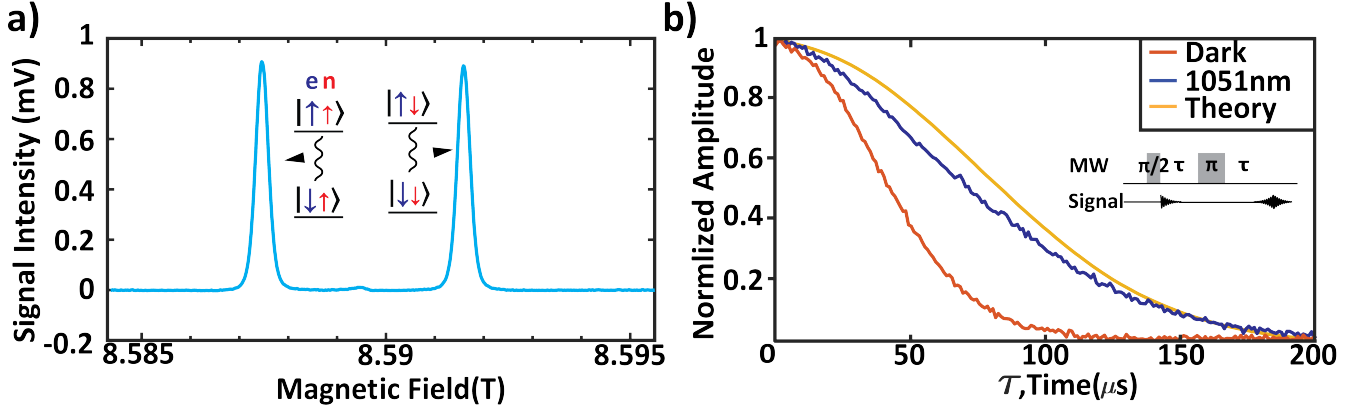


FIG. 1: (a) cw-ESR spectrum of the bulk Si:P sample at 4.3 K showing the 2 hyperfine-split transitions. We refer to the two peaks as the high-field and low-field peaks. The spectra are obtained under fast-passage conditions with a 40 kHz modulation frequency and 0.1 mT modulation strength. The microwave power is 20 μ W. (b) Two Hahn echo decays acquired back to back on the high field transition. The x-axis is the τ time between the two microwave pulses. The blue curve shows the Hahn echo decay signal acquired under 1051 nm light excitation. The red curve is the Hahn echo decay signal acquired without any light excitation. The green curve is the theoretical prediction from the pair correlation approach of Witzel *et al.* which was found to be in excellent agreement with low-field experiments.

includes contributions from instantaneous diffusion (ID), spectral diffusion (SD) and the T_2 coherence time of the spins [11]. In silicon the parameter n has been observed to be in the range from 2–3 [3]. Instantaneous diffusion describes the decay observed due to dipolar-induced spin-flips with surrounding electron spins that are also excited by the microwave pulse. For 10^{15} electron spins/cm³ the characteristic time T_{ID} for instantaneous diffusion is about 1.2 ms [11]. At high fields the T_1 relaxation time is known to shorten considerably and has been measured to be on the order of 20 ms in the dark in a similarly doped sample [23]. In the absence of coupling to other spins – which is accounted for by the instantaneous diffusion and spectral diffusion terms – we expect $T_2 \sim T_1 \sim 20$ ms. T_2 and T_{ID} are thus both significantly longer than the timescales on which the decays are observed and do not play a significant role in these experiments. Fitting the echo decays to the spectral diffusion component of Equation [2] using $n = 2.3$ as measured both theoretically [8] and experimentally [3] for Si:P, we obtain $T_{SD} = 124 \pm 7$ μ s in the dark and $T_{SD} = 201 \pm 11$ μ s under 1051 nm excitation. At low field T_{SD} was found to range from 270 μ s to 620 μ s depending on the orientation of crystal in the magnetic field [3]. The T_{SD} observed in the dark is thus more than a factor 2 smaller than that measured at lower magnetic fields. Under optical excitation T_{SD} is seen to increase and is closer to the value of T_{SD} measured in the dark at low magnetic fields. Figure 1(b) also shows the simulated echo decay calculated using the pair correlation approach of Witzel *et al.* which was found to be in excellent agreement with low-field experiments [8, 9].

In an effort to better understand these surprising experimental results, it is useful to examine the microscopic

origins of the T_{SD} variations. Following [8–10, 25, 26] we can cast this problem in terms of a qubit-bath Hamiltonian with the donor electron as the spin qubit and the nuclear spins as the bath. Since we are exploring the coherence properties of a single ESR manifold, we can treat this as a single spin and ignore the donor nucleus. The Hamiltonian describing the interaction of this electron spin with the surrounding ²⁹Si spins can be expressed as

$$H = \omega_e S_z + S_z \sum_i A_i I_z^i + \omega_n \sum_i I_z^i + \sum_{i < j} h_{ij} \quad (3)$$

consisting of the electron Zeeman, electron-nuclear hyperfine, nuclear Zeeman and nuclear dipolar interactions respectively. The pairwise nuclear dipolar interaction is given by $h_{ij} = d_{ij} (I_x^i I_x^j + I_y^i I_y^j - 2I_z^i I_z^j)$, where $d_{ij} = (\gamma_n^2 / 2r_{ij}^3) (3 \cos^2 \theta_{ij} - 1)$.

The hyperfine interactions A_i contain both contact and dipolar contributions. The electron and nuclear Zeeman interaction terms can be dropped as they independently commute with all other terms in the Hamiltonian and play no role in the decay of the electron spin coherence in a Hahn-echo experiment. The qubit-bath Hamiltonian can be re-written as

$$\mathcal{H} = |\uparrow\rangle\langle\uparrow| \otimes H^+ + |\downarrow\rangle\langle\downarrow| \otimes H^- \quad (4)$$

where $H^\pm = \pm \frac{1}{2} \sum_i A_i I_z^i + \sum_{i < j} h_{ij}$ are different bath Hamiltonians that depend on the qubit state ($|\uparrow\rangle$ or $|\downarrow\rangle$) [10]. If the bath nuclear spins are initially in a state $|J\rangle$ – a random thermal equilibrium nuclear spin configuration, then an initial coherent superposition state of the qubit

$$|\psi(0)\rangle = (\alpha|\uparrow\rangle + \beta|\downarrow\rangle) \otimes |J\rangle \quad (5)$$

evolves into a state

$$\psi(t)\rangle = \alpha|\uparrow\rangle \otimes e^{-iH^+t}|J\rangle + \beta|\downarrow\rangle \otimes e^{-iH^-t}|J\rangle \quad (6)$$

at time t , entangling the spin and bath. Evaluating the state of the spins at time $t = 2\tau$ in a Hahn echo experiment and tracing over the nuclear spins gives us the magnitude of the electron spin echo

$$S(2\tau) = \langle J|e^{iH^-\tau}e^{iH^+\tau}e^{-iH^-\tau}e^{-iH^+\tau}|J\rangle \quad (7)$$

For a mixed state of the nuclear spin bath $\rho = \sum_J p_J|J\rangle\langle J|$, we average equation [7] over the different bath states. The magnetic field dependence of this expression for the spectral diffusion only arises from the probabilities for the different bath configurations. At $T = 4$ K and $B = 8.58$ T we have a thermal equilibrium ^{29}Si nuclear spin polarization of 4.4×10^{-4} which indicates that the nuclear spins are effectively at infinite temperature and all bath configurations are equally likely. The resulting echo amplitude

$$S(2\tau) = \text{Tr} \left[e^{iH^-\tau}e^{iH^+\tau}e^{-iH^-\tau}e^{-iH^+\tau} \right] \quad (8)$$

is independent of magnetic field in contrast to our experimental result, as long as the Hamiltonian parameters of the system remain unchanged.

Different approaches have been used to estimate the decay due to this many-body dynamic [10]. For a 2-pulse spin echo experiment the pair correlation function approach has been shown to give very good agreement to experimental results at low magnetic fields [8, 9]. The resulting echo intensity is

$$S(2\tau) = \exp \left(- \sum_{i < k} \frac{d_{ij}^2(A_i - A_j)^2}{4\omega_{ij}^4} [\cos \omega_{ij}\tau - 1]^2 \right) \quad (9)$$

where $\omega_{ij} = \frac{1}{2}\sqrt{(A_i - A_j)^2 + 4d_{ij}^2}$. Figure 1(b) compares numerical simulations of this model to the experimental data acquired at high field. The simulated curve has been multiplied by an decaying exponential to account for instantaneous diffusion effects ($T_{\text{ID}} = 1.2$ ms). Details of the simulation are provided in the Supplementary Information.

Ultimately the observed changes in T_{SD} indicate changes in the local magnetic field fluctuations seen by the donor electron. The decrease in T_{SD} in the dark suggests that either the magnitude of the magnetic noise has increased or that the fluctuations have become more rapid leading to imperfect refocusing by the spin echo. One possibility is that the Kohn-Luttinger wavefunctions [27, 28] are perturbed by the high-field conditions used here so that the magnitudes of the ^{29}Si hyperfine interactions become larger, thus increasing the strength of the magnetic noise seen by the electron spin. While the ESR conditions are a sensitive probe of the phosphorus donor

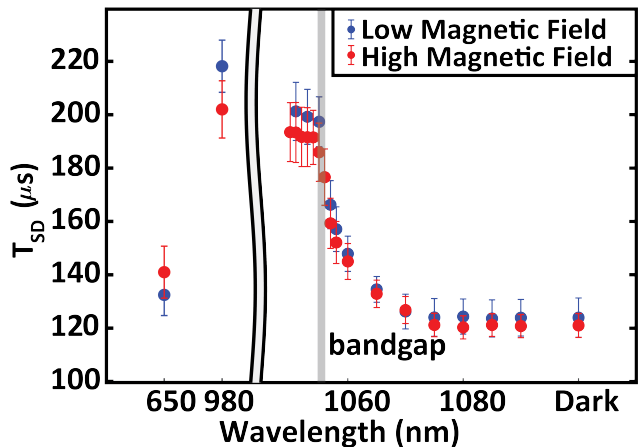


FIG. 2: The change in T_{SD} as a function of optical excitation wavelength for ESR experiments run at both the low-field and high-field phosphorus peaks of Figure 1(b). The high magnetic field data was collected in 1 nm steps between 1050 nm and 1060 nm while the low magnetic field data was collected at 1051 nm, 1053 nm, 1055 nm, 1057 nm, 1058 nm and 1060 nm.

hyperfine interaction strength and were not observed to change under optical excitation, they do not tell us about the ^{29}Si hyperfine coupling strengths, which would require electron-nuclear double resonance (ENDOR) experiments under the same conditions.

In order to further understand the enhancement of spectral diffusion time under light excitation, we repeated the experiment with a tunable laser (O/E Land OETLS-300-1060 electrically-tunable external-cavity fiber laser) that could be tuned across the band edge from 1050 nm to 1090 nm (corresponding to the energy window 1.1375 – 1.18 eV). Silicon is an indirect band-gap material with a band-gap of 1.17 eV at 4.2 K [29]. The first optical absorption edge at $E = 1.174$ eV (1056 nm) is mediated by the emission of 18.2 meV TA phonons and the creation of a free exciton [30]. The power of the tunable laser varies between 250 μW and 2 mW - depending on the wavelength as shown in the Supplementary Materials. The optical linewidth is specified to be below 0.04 nm. We also ran the experiment with 650 nm ($E = 1.91$ eV) and 980 nm ($E = 1.27$ eV) excitation, using free space lasers coupled into the fiber.

Figure 2 shows the measured spectral diffusion time at different laser wavelength for both the high-field and the low-field phosphorus peaks of Figure 1(b). The signal decays are fit to just the T_{SD} term using $n = 2.3$. The error bars are calculated by the 95 percent confidence interval of the T_{SD} . The data show that T_{SD} increases as the energy of the optical excitation is increased above the silicon band-gap, and that the change in spectral diffusion time is the same for both the high-field and low-field phosphorus peaks. The longer T_{SD} is also observed with the 980 nm laser, but falls off again at 650 nm, likely

due to the limited penetration depth into the sample. It should be noted that the signal measured in these inductively detected pulsed ESR experiments arises from the entire sample. At cryogenic temperatures the optical penetration depth of light into silicon is known to be strongly wavelength dependent [31]. For wavelengths of 1050 nm and longer the optical penetration depth is several centimeters, while it reduces to about $100 \mu\text{m}$ at 980 nm and to 2-3 μm at 650 nm. Thus the 3 mm thick sample is expected to be uniformly illuminated at the longer wavelengths, fairly inhomogeneously illuminated at 980 nm and only the very surface of the sample is optically excited by the 650 nm wavelength. The photo-excited carriers can travel further into the sample, with free excitons traveling up to a millimeter in silicon under these conditions [32].

Figure 3 shows the change in T_{SD} as a function of nominal laser power (measured at the output of the optical fiber) with the 980 nm laser for the high magnetic field transition. The fit indicates that T_{SD} saturates to a maximum of $208 \mu\text{s}$ with increasing laser power. This is close to the value measured at low magnetic fields.

The increase in T_{SD} indicates either that the magnitude of the noise reduces, or the spectral features change – either slowing down and enabling better refocusing by the spin echo or fluctuating rapidly enough to enable a “motional narrowing” of the noise [33]. For NV centers in diamond, polarizing the spin bath (electronic P1 centers) has been shown to suppress spectral diffusion and increase T_{SD} [34]. While above bandgap illumination has been shown to hyperpolarize the phosphorus donor spins at high field and low temperature [21, 35, 36], only weak optical hyperpolarization of the silicon spins has been observed to date at high magnetic fields [24]. Verhulst *et al.* observed a ^{29}Si spin polarization of 0.25% at 500 mW after 30 minutes of laser irradiation at 7 T and 4.2 K. With 1024.8 nm excitation, they initially observed a reduction in T_1 of the silicon spins at low optical power ($< 1 \text{ mW}$) and a growth of ^{29}Si hyperpolarization at higher optical power ($> 1 \text{ mW}$). The 1-2 mW optical power coming out of the fiber in our experiments is just on the threshold of when ^{29}Si hyperpolarization was observed, so it is unlikely that the ^{29}Si nuclear spins polarization is sufficiently high to change T_{SD} significantly. More importantly, given the long T_1 of the silicon nuclear spins, the enhanced T_{SD} should persist for several hours. However, as shown in Figure 1(b), the enhanced spectra diffusion times were not observed when the experiment was repeated in the dark 15 minutes later.

Alternatively, spectral diffusion effects can also be reduced if the effective strength of either the inter-nuclear dipolar coupling or the hyperfine coupling are reduced or acquire rapid random rapid fluctuations that lead to motional narrowing of the local field fluctuations. One possibility is that modulation of the donor electron wavefunction by mobile carriers modulates and reduces the silicon

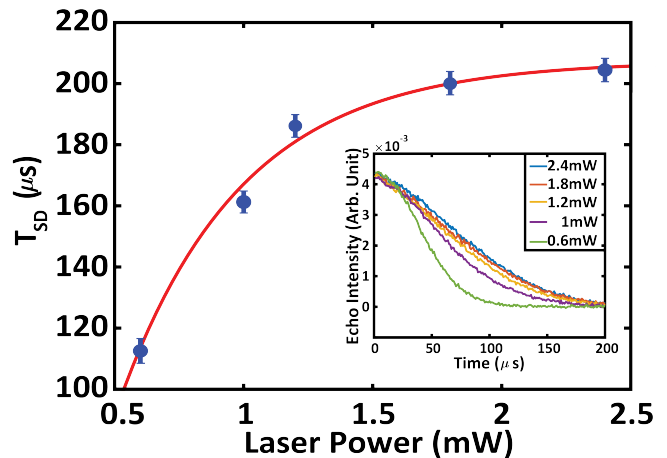


FIG. 3: T_{SD} as a function of laser power with 980 nm laser excitation on the high magnetic field transition. The red line is a fit to the saturation function $T(1 - \exp(-\alpha(P - P_0)))$, yielding $T = 207.7 \mu\text{s}$ as the saturation value. The inset shows the echo intensity decay at various laser powers.

hyperfine couplings. While noise spectroscopy [37, 38] could be used in principle to directly measure the spectrum of magnetic noise seen by the donors, the lack of phase control on the 240 GHz instruments does not permit robust multiple-pulse dynamical decoupling experiments. Disentangling the different potential sources of magnetic field fluctuations in the presence of light is a non-trivial task. Optical excitation creates a dynamically rich environment for the spins as can be seen from the schematic in Figure 4.

At the absorption edge, the electrons and holes are primarily in the form of free excitons (the exciton binding energy is $15.01 \pm 0.06 \text{ meV}$ [30]), while at higher optical excitation energies above 1.19 eV, it is possible to generate free electrons and holes - which in turn form free excitons as they lose energy. The optical generation of free excitons is followed by continuous interconversion between free and bound excitons, and both radiative recombination of free excitons and non-radiative Auger recombination of bound excitons [39]. A 1 mW excitation with 1 eV photons would result in 6.25×10^{15} photoelectrons/excitons generated per second if all the power is deposited in the sample. Given the penetration depth of 1 eV photons in silicon only about 10% of the photons are absorbed. Since the free exciton lifetime at 4.2 K is on the order of $1 \mu\text{s}$ [39], this results in an estimated exciton density of about $8 \times 10^9 \text{ cm}^{-3}$ in the sample - significantly lower than the donor concentration. However, the excitonic Bohr radius is about 5 nm [40] - larger than that of the donor electron - and they are known to have extremely high mobilities [32]. It is possible that that exciton dynamics contributes to the observed increase in T_{SD} as the electrons and holes comprising these excitons can have fairly strong hyperfine couplings to the silicon

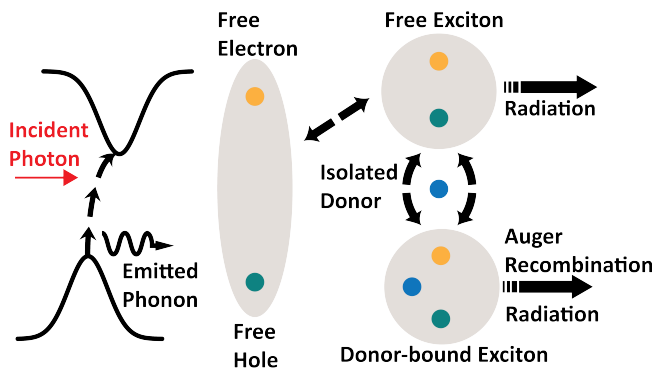


FIG. 4: Schematic of the effects following optical absorption in silicon.

nuclei in the lattice [41].

In conclusion, the spectral diffusion time measured in the dark at high field (8.59 T) was observed to be more than a factor of 2 shorter than the values measured at 0.35 T, though the simple theory outlined here would suggest that the values should be identical. In the presence of weak above band-gap optical excitation, T_{SD} was observed to increase by almost a factor of 2 suggesting a motional narrowing of the spectrum of magnetic field fluctuations seen by the donor.

ACKNOWLEDGEMENTS

We thank William Coish and Susumu Takahashi for helpful discussions. This work was supported in part by the National Science Foundation under grants OIA-1921199. Part of the work was done at the National High Magnetic Field Laboratory, which is supported by the NSF under grant DMR-1644779 and the State of Florida.

* sekhar.ramanathan@dartmouth.edu

- [1] D. D. Awschalom, L. C. Bassett, A. S. Dzurak, E. L. Hu, and J. R. Petta, *Science* **339**, 1174 (2013).
- [2] D. D. Awschalom, R. Hanson, J. Wrachtrup, and B. B. Zhou, *Nature Photonics* **12**, 516 (2018).
- [3] A. M. Tyryshkin, J. J. L. Morton, S. C. Benjamin, A. Ardavan, G. A. D. Briggs, J. W. Ager, and S. A. Lyon, *J Phys-Condens Mat* **18**, S783 (2006).
- [4] A. M. Tyryshkin, S. Tojo, J. J. L. Morton, H. Riemann, N. V. Abrosimov, P. Becker, H.-J. Pohl, T. Schenkel, M. L. W. Thewalt, K. M. Itoh, et al., *Nature Materials* **11**, 143 (2011).
- [5] R. de Sousa and S. Das Sarma, *Phys. Rev. B* **68**, 115322 (2003).
- [6] W.-L. Ma, G. Wolfowicz, N. Zhao, S.-S. Li, J. J. Morton, and R.-B. Liu, *Nat Commun* **5**, 4822 (2014).
- [7] W.-L. Ma, G. Wolfowicz, S.-S. Li, J. J. L. Morton, and R.-B. Liu, *Phys. Rev. B* **92**, 161403 (2015).
- [8] W. M. Witzel and S. Das Sarma, *Phys. Rev. B* **74**, 035322 (2006).
- [9] W. M. Witzel, X. Hu, and S. Das Sarma, *Phys. Rev. B* **76**, 737 (2007).
- [10] W. Yang, W.-L. Ma, and R.-B. Liu, *Rep. Prog. Phys.* **80**, 016001 (2017).
- [11] A. Schweiger and G. Jeschke, *Principles of pulse electron paramagnetic resonance* (Oxford, 2001).
- [12] A. Morello, J. J. Pla, F. A. Zwanenburg, K. W. Chan, K. Y. Tan, H. Huebl, M. Mottonen, C. D. Nugroho, C. Yang, J. A. van Donkelaar, et al., *Nature* **467**, 687 (2010).
- [13] J. J. Pla, K. Y. Tan, J. P. Dehollain, J. J. L. Lim, W. H. and Morton, D. N. Jamieson, A. S. Dzurak, and A. A. Morello, *Nature* **489**, 541 (2012).
- [14] J. T. Muhonen, J. P. Dehollain, A. Laucht, F. E. Hudson, R. Kalra, T. Sekiguchi, K. M. Itoh, D. N. Jamieson, J. C. McCallum, A. S. Dzurak, et al., *Nature nanotechnology* **9**, 986 (2014).
- [15] M. Veldhorst, C. Yang, J. Hwang, W. Huang, J. Dehollain, J. Muhonen, S. Simmons, A. Laucht, F. Hudson, K. M. Itoh, et al., *Nature* **526**, 410 (2015).
- [16] Y. He, S. K. Gorman, D. Keith, L. Kranz, J. G. Keizer, and M. Y. Simmons, *Nature* **571**, 371 (2019).
- [17] J. van Tol, L.-C. Brunel, and R. J. Wyde, *Review of Scientific Instruments* **76**, 074101 (2005).
- [18] C. P. Slichter, *Phys. Rev.* **99**, 479 (1955).
- [19] A. E. Dementyev, D. G. Cory, and C. Ramanathan, *J. Chem. Phys.* **134** (2011).
- [20] G. Morley, D. McCamey, and H. Seipel, *Phys. Rev. Lett.* **101**, 207602 (2008).
- [21] D. R. McCamey, J. van Tol, G. W. Morley, and C. Boehme, *Phys. Rev. Lett.* **102**, 027601 (2009).
- [22] D. R. McCamey, J. van Tol, G. W. Morley, and C. Boehme, *Science* **330**, 1652 (2010).
- [23] D. R. McCamey, C. Boehme, G. W. Morley, and J. van Tol, *Phys. Rev. B* **85**, 073201 (2012).
- [24] A. S. Verhulst, I. G. Rau, Y. Yamamoto, and K. M. Itoh, *Phys. Rev. B* **71**, 235206 (2005).
- [25] W. Yang and R.-B. Liu, *Phys. Rev. B* **78**, 935 (2008).
- [26] W. M. Witzel, M. S. Carroll, A. Morello, L. Cywinski, and S. Das Sarma, *Phys. Rev. Lett.* **105**, 187602 (2010).
- [27] W. Kohn and J. M. Luttinger, *Phys. Rev.* **97**, 883 (1955).
- [28] W. Kohn and J. M. Luttinger, *Phys. Rev.* **98**, 915 (1955).
- [29] M. A. Green, *Journal of Applied Physics* **67**, 2944 (1990).
- [30] M. A. Green, *AIP Advances* **3**, 112104 (2013).
- [31] G. G. Macfarlane, T. P. McLean, J. E. Quarrington, and V. Roberts, *Physical Review* **111**, 1245 (1958).
- [32] M. A. Tamor and J. P. Wolfe, *Phys. Rev. Lett.* **44**, 1703 (1980).
- [33] J. R. Klauder and P. W. Anderson, *Phys Rev* **125**, 912 (1962).
- [34] S. Takahashi, R. Hanson, J. van Tol, M. S. Sherwin, and D. D. Awschalom, *Phys. Rev. Lett.* **101**, 047601 (2008).
- [35] P. Gumann, O. Patange, C. Ramanathan, H. Haas, O. Moussa, M. L. W. Thewalt, H. Riemann, N. V. Abrosimov, P. Becker, H. J. Pohl, et al., *Phys. Rev. Lett.* **113**, 267604 (2014).
- [36] P. Gumann, H. Haas, S. Sheldon, L. Zhu, R. Deshpande, T. Alexander, M. L. W. Thewalt, D. G. Cory, and C. Ramanathan, *Phys. Rev. B* **98**, 180405 (2018).
- [37] G. A. Álvarez and D. Suter, *Phys. Rev. Lett.* **107**, 230501 (2011).

- [38] J. Bylander, S. Gustavsson, F. Yan, F. Yoshihara, K. Harrabi, G. Fitch, D. G. Cory, Y. Nakamura, J.-S. Tsai, and W. D. Oliver, *Nature Phys* **7**, 565 (2011).
- [39] R. B. Hammond and R. N. Silver, *Appl. Phys. Lett.* **36**, 68 (1980).
- [40] T. McLean and R. Loudon, *Journal of Physics and Chemistry of Solids* **13**, 1 (1960).
- [41] P. Philippopoulos, S. Chesi, and W. A. Coish, *Phys. Rev. B* **101**, 115302 (2020).